Ludwig Maximilians Universität München

Multiple-scattering formalism for correlated systems: A KKR-DMFT approach

H. Ebert, J. Minár, D. Ködderitzsch

Ludwig-Maximilians-Universität München,
Department Chemie - Lehrbereich Phys. Chemie
Butenandtstraße 11, D-81377 MÜnchen

In close collaboration with

A. Lichtenstein [1], M. Katsnelson [2], L. Chioncel [3]

[1] University Hamburg, Germany
[2] University Nijmegen, Netherlands
[3] University Augsburg, Germany

and many experimental colleagues

Outline

- Introduction
- The standard LSDA+DMFT implementation
- Combination of LSDA+KKR
  - single site problem
  - multiple scattering
- Electronic properties and relativistic extension
- Disordered Alloys
- Applications
  - Magnetic moments
  - Total energy
  - spectroscopy
- Summary

Dynamical mean field theory (DMFT)

- DMFT maps a lattice many-body system onto multi-orbital Anderson-like impurity model (AIM)

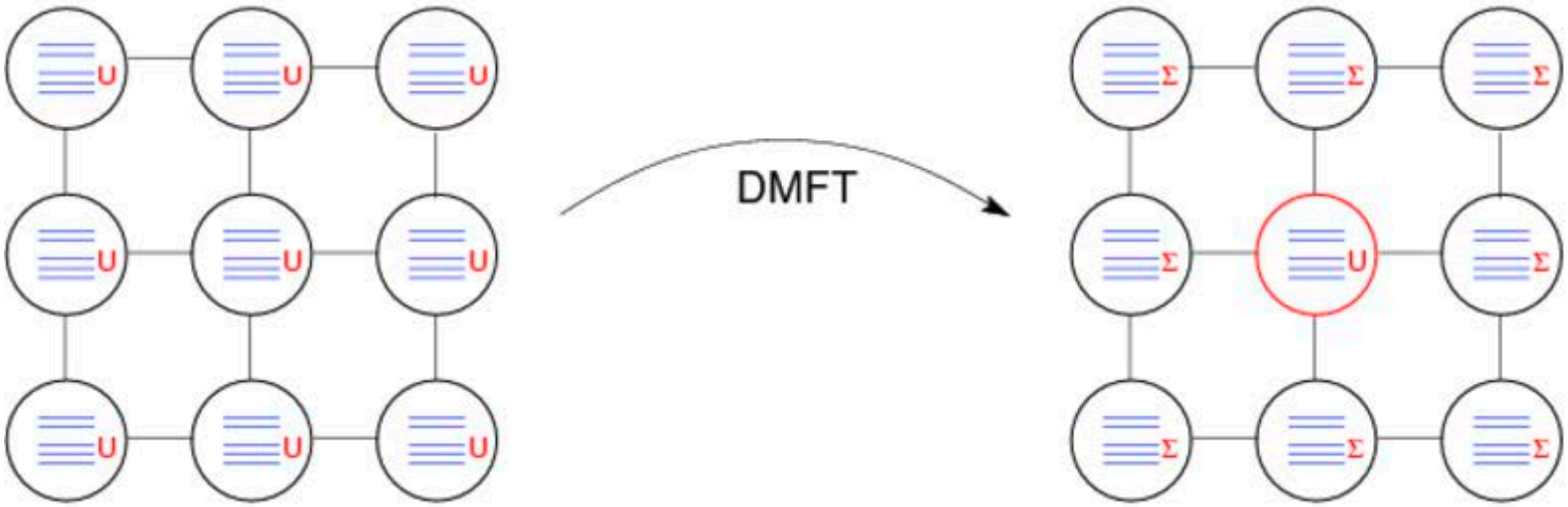

- Metzner, Vollhardt, PRL '89, simplification for $d \to \infty$
- Georges, Kotliar, PRB '92, mapping onto a AIM
- Anisimov et al., EPJ '97, LDA+DMFT

Combined LSDA+DMFT Hamiltonian

$$H = H_{\mathrm{LSDA}} + \Big[\frac{1}{2} \sum_{il} {\sum_{m\sigma\, m'\sigma'}}' U^{\sigma\sigma'}_{mm'} \hat{n}_{ilm\sigma} \hat{n}_{ilm'\sigma'} - \frac{1}{2} \sum_{il} {\sum_{m\sigma\, m'}}' J_{mm'} \hat{c}^{\dagger}_{ilm\sigma} \hat{c}_{ilm'\bar{\sigma}} \hat{c}^{\dagger}_{ilm'\bar{\sigma}} \hat{c}_{ilm\sigma} - \sum_{il} \sum_{m\sigma} \Delta\epsilon_l \hat{n}_{ilm\sigma} \Big]_{i=i_d, l=d}$$

- $U^{\uparrow\downarrow}_{mm'} = U \quad U^{\sigma\sigma'}_{mm'} = U - 2J - J\delta_{\sigma\sigma'}$

  U intra-orbital Coulomb repulsion

  from constrained LSDA or linear response
- J Hund exchange term
- $\Delta\varepsilon$ double counting corrections

Standard DMFT scheme (e.g. LMTO)

SCF-cycle

LSDA Green's function in reciprocal space

$$G_{\mathrm{LSDA}}(k,E) = [E - H_{\mathrm{LSDA}}(k)]^{-1}$$

AIM: Dyson-equation for LSDA+DMFT Green's function

$$G^{-1}(k,E) = G^{-1}_{\mathrm{LSDA}}(k,E) - \Sigma(E)$$

LSDA+DMFT single particle Green's function

$$G(E) = \Omega^{-1} \int \mathrm{d}^3k \; G(k,E)$$

Effective medium or bath Green's function

$$\mathcal{G}^{-1}(E) = G^{-1}(E) + \Sigma(E)$$

DMFT-solver: $\boxed{G_{\mathrm{new}} = G[\mathcal{G}]} \quad \Rightarrow \quad \Sigma_{\mathrm{new}}(E) = \mathcal{G}^{-1}(E) - G^{-1}(E)$

LSDA: $G(E) \rightarrow \rho(E) \rightarrow V_{\mathrm{LSDA}} \rightarrow H_{\mathrm{LSDA}}$

Electronic self-energy Σ

one-particle Green's function $\hat{G}$

$$\left[E - \hat{H}_{LSDA} - \hat{\Sigma}(E)\right]\hat{G} = \hat{1}$$

effective self-energy operator

$$\hat{\Sigma}(E) = \sum_{ij} |\phi_{ni}\rangle \Sigma_{ij}(E) \langle\phi_{nj}|$$

assumed to be site diagonal

$|\phi_{ni}\rangle$ localized orbitals for lattice site n

Spin-dependent self-energy matrix for fcc-Ni

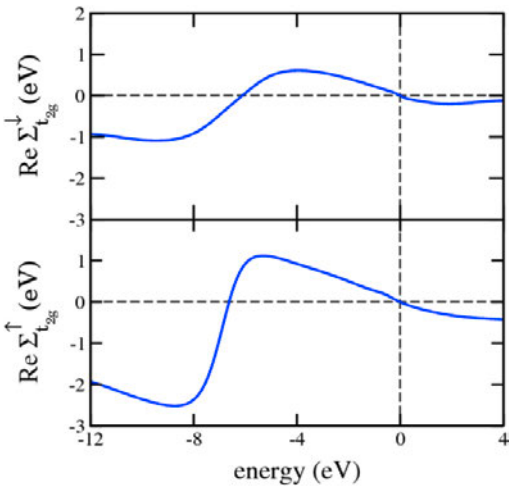

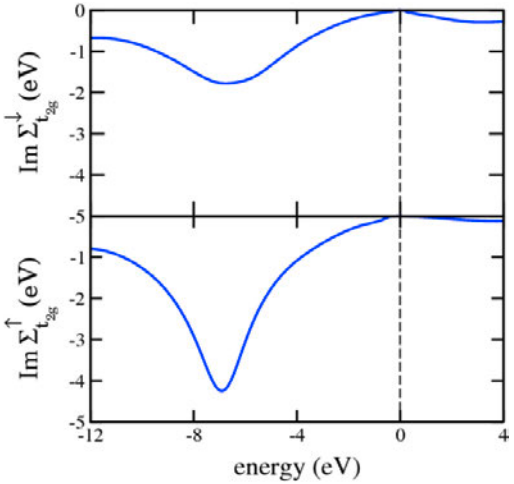

Green's function based methods

One-electron Green's function in terms of eigen values E_i and eigen functions $\phi_i(\vec{r})$

$$G^+(\vec{r},\vec{r}',E) = \lim_{\epsilon\to 0}\sum_i \frac{\phi_i(\vec{r})\phi_i^*(\vec{r})}{E-E_i+i\epsilon}$$

- Dyson equation $G = G_0 + G\Delta\mathcal{H}G_0$
  - linear response formalism
  - treatment of complex structures:

    surfaces, nano-structures
- CPA alloy theory
- description of spectroscopic quantities
- central quantity of many-body theories

Implementation of LSDA+DMFT using Green's function methods

Dyson equation for one-electron Green's function

$$G(\vec{r},\vec{r}\,',E) = G_0(\vec{r},\vec{r}\,',E) + \int \mathrm{d}^3r'' \int \mathrm{d}^3r''' G_0(\vec{r},\vec{r}\,'',E) \left[V_{\mathrm{LSDA}}(\vec{r}\,'')\delta(\vec{r}\,''-\vec{r}\,''') + \Sigma(\vec{r}\,'',\vec{r}\,''',E)\right] G(\vec{r}\,''',\vec{r}\,',E)$$

$G_0(\vec{r},\vec{r}\,',E)$ free electron Green's function

$\Sigma(\vec{r},\vec{r}\,',E)$ self-energy

Approximation: $\Sigma(\vec{r},\vec{r}\,',E)$ is site-diagonal

Densities and expectation values

The Dirac identity $\lim_{\epsilon \to 0} \Im \frac{1}{x + i\epsilon} = -\pi \, \delta(x)$ leads to

$$-\frac{1}{\pi} \Im G^{+}(\vec{r}, \vec{r}\,', E) = \sum_i \psi_i(\vec{r}) \psi_i^{\times}(\vec{r}\,') \delta(E - E_i)$$

$\Im G^{+}(\vec{r}, \vec{r}\,', E)$ can be interpreted as density matrix

Density of states $$n(E) = -\frac{1}{\pi} \Im \int_V d^3r \, G^{+}(\vec{r}, \vec{r}, E)$$

Particle density $$n(\vec{r}) = -\frac{1}{\pi} \Im \int^{E_F} dE \, G^{+}(\vec{r}, \vec{r}, E)$$

Expectation value $$\langle \mathcal{A} \rangle = -\frac{1}{\pi} \Im \int^{E_F} dE \int_V d^3r \, \mathcal{A} G^{+}(\vec{r}, \vec{r}, E)$$

One-electron Green's function via KKR formalism

Electronic structure represented by **Green's function**

$$G^{+}(\vec{r},\vec{r}',E) = \lim_{\epsilon\to 0}\sum_{i}\frac{\phi_i(\vec{r})\phi_i^{\times}(\vec{r}')}{E-E_i+i\epsilon}$$

Korringa-Kohn-Rostoker (**KKR**) method
based on multiple scattering theory

$$G^{+}(\vec{r},\vec{r}',E) = \sum_{L,L'} Z_L(\vec{r},E)\tau^{nm}_{LL'}(E)Z^{\times}_{L}(\vec{r}',E) - \delta_{nm}\sum_{L} Z_L(\vec{r}_<,E)J^{\times}_{L}(\vec{r}_>,E)$$

$Z\ (J)$	regular (irregular) solution of Schrödinger equation
τ	scattering path operator
$L=(l,m_l)$	angular momentum quantum numbers

Multiple scattering (KKR) formalism

Solve Dyson equation

$$\mathcal{G} = \mathcal{G}_0 + \mathcal{G}_0 V \mathcal{G}$$
$$= \mathcal{G}_0 + \mathcal{G}_0 \mathcal{T} \mathcal{G}_0$$

for scattering operator

$$\mathcal{T} = \sum_{n,m} \tau^{nm}$$

scattering path operator

$$\tau^{nm} = t^n \delta_{nm} + \sum_{k \neq n} t^n \mathcal{G}_0 \, \tau^{km}$$

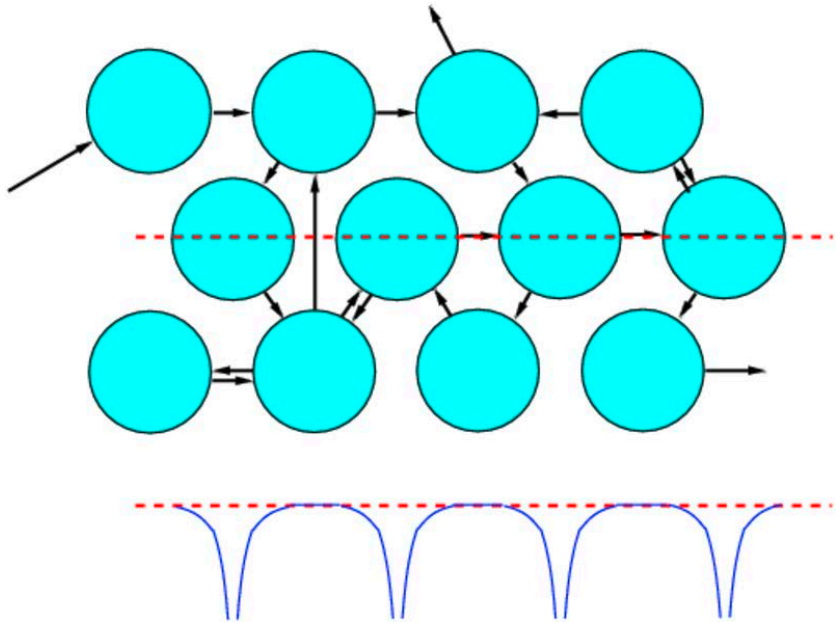

single-site scattering matrix t^n

free electron Green's function $\mathcal{G}_0$

KKR single-site problem

$$[-\nabla^2 + V^\sigma(r) - E]\Psi(\vec{r}) + \int \Sigma^\sigma(\vec{r},\vec{r}',E)\Psi(\vec{r}')d^3r = 0$$

Ansatz: $\Psi(\vec{r}) = \sum_L \Psi_L(\vec{r})$

$$\left[\frac{d^2}{dr^2} - \frac{l(l+1)}{r^2} - V(r) + E\right]\Psi_L(r,E) =$$

$$\sum_{L''} \int r'^2 dr' \Sigma_{LL''}(E)\,\phi_l(r)\phi_{l''}(r')\Psi_L(r',E)$$

Approximation for the self-energy:

$$\sum_L \int d^3r' \phi^\dagger_{L'}(\vec{r})\Sigma_{L'L}(E)\phi_L(\vec{r}\,')\Psi_L(\vec{r}\,',E) \approx \sum_L \Sigma_{L'L}(E)\Psi_L(\vec{r},E)$$

Pure differential equation:

$$\left[\frac{d^2}{dr^2} - \frac{l(l+1)}{r^2} - V(r) + E\right]\Psi_L(r,E) = \sum_{L'} \Sigma_{LL'}(E)\,\Psi_{L'}(r,E)$$

Angular momentum representation for $\tau^{nm}(E)$

$$\tau^{nm}_{LL'}(E) = \int_{\Omega_n} \mathrm{d}3r_n \int_{\Omega_m} \mathrm{d}3r'_m j^{\times}_L(\vec{r}_n, E)\langle \vec{r}_n|\tau^{nm}|\vec{r}\,'_m\rangle j_{L'}(\vec{r}_m\,', E)$$

corresponding equation of motion

$$\underline{\tau}^{nm}(E) = \underline{t}^{n}(E)\delta_{nm} + \underline{t}^{n}(E)\sum_{k\neq n}\underline{G}^{nk}_{0}(E)\underline{\tau}^{km}(E)$$

and

$$[\underline{\tau}^{nm}]_{LL'} = \tau^{nm}_{LL'}$$
$$[\underline{G}^{nm}_{0}]_{LL'} = G^{nm}_{0\,LL'}(1-\delta_{nm})$$
$$[\underline{t}^{n}]_{LL'} = t^{n}_{l}\delta_{LL'}$$

matrix dimension: $\sum_{l=0}^{l_{\max}}\sum_{m=-l}^{+l} 1 = (l_{\max}+1)2$

Calculating τ^{nm} for finite array of scatterers

$$\underline{\underline{\tau}}(E) = \underline{\underline{t}}(E) + \underline{\underline{t}}(E)\,\underline{\underline{G}}_0(E)\,\underline{\underline{\tau}}(E)$$

with

$$\begin{aligned} \left[\underline{\underline{\tau}}\right]^{nm} &= \underline{\underline{\tau}}^{nm} \\ \left[\underline{\underline{t}}\right]^{nm} &= \underline{\underline{t}}^{n}\delta_{nm} \\ \left[\underline{\underline{G}}_0\right]^{nm} &= \underline{\underline{G}}_0^{nm}(1-\delta_{nm}) \end{aligned}$$

$$\boxed{\underline{\underline{\tau}}(E) = \left[\underline{\underline{t}}(E)^{-1} - \underline{\underline{G}}_0(E)\right]^{-1}}$$

matrix dimension: $\mathbf{N_{scatterers}} \times (l_{\max}+1)2$

KKR Green's function matrix

Green's function matrix $G^{nm}_{LL'}$ within KKR-formalism

$$G^{nm}_{LL'}(E) = \sum_{L_1,L_2} \langle \phi_L \mid Z_{L_1} \rangle \tau^{nm}_{LL'}(E) \langle Z^{\times}_{L_2} \mid \phi_{L'} \rangle$$

$$- \delta_{nm} \sum_{L_1} \langle \phi_L \mid Z_{L_1}(\mathrm{r}_<, E) J^{\times}_{L_1}(\mathrm{r}_>, E) \mid \phi_{L'} \rangle$$

$G^{nn}_{LL'}$ — input for the many-body effective impurity problem

$\phi_L(\vec{r})$ — basis function solution of the Schrödinger equation for spherical LSDA non-magnetic potential

KKR+DMFT scheme

SCF cycle

$\mathbf{V_{LSDA}}(\vec{r})$ $\quad$ $\boldsymbol{\Sigma}(E)$

$\Downarrow$

single-site problem: $t_{LL'}(E)$

$\Downarrow$

multiple scattering: $\tau_{LL'}(E)$

$\Downarrow$

KKR-Green's function: $G(\vec{r},\vec{r}\,',E)$

$\Downarrow$ $\quad$ $\Downarrow$

charge $\rho(\vec{r})$ $\quad$ G-matrix $G_{LL'}(E)$

$\Downarrow$ $\quad$ $\Downarrow$

LSDA $\quad$ DMFT-solver

$\Downarrow$ $\quad$ $\Downarrow$

$\mathbf{V_{LSDA}}(\vec{r})$ $\quad$ $\boldsymbol{\Sigma}(E)$

CPA

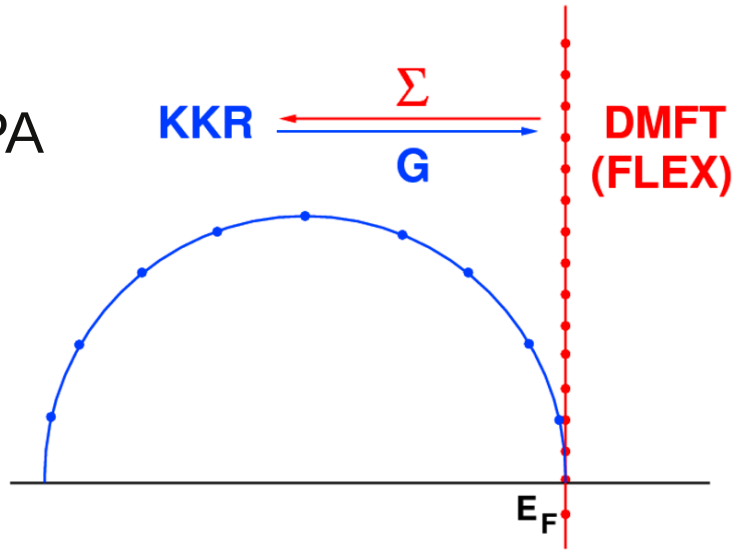

LSDA+DMFT applied to fcc Ni

Density of states

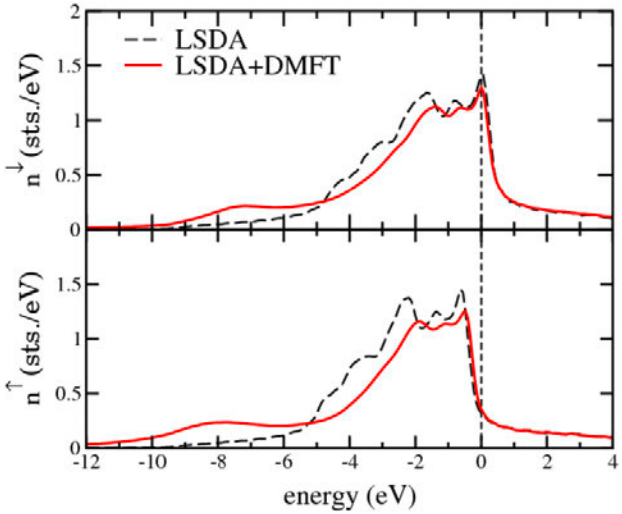

	μ_{spin}
LSDA	0.563
LSDA+DMFT	0.569

Self-energy

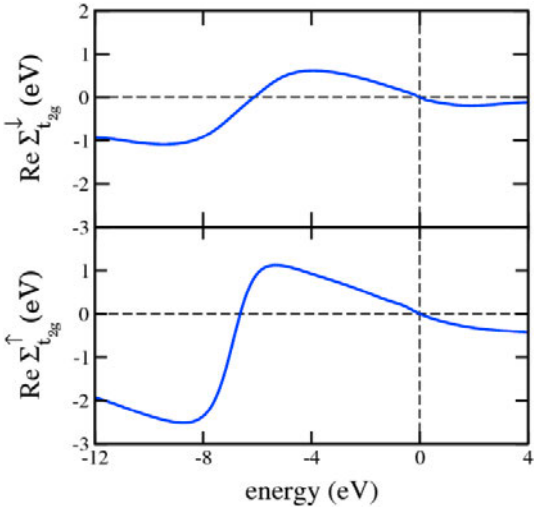

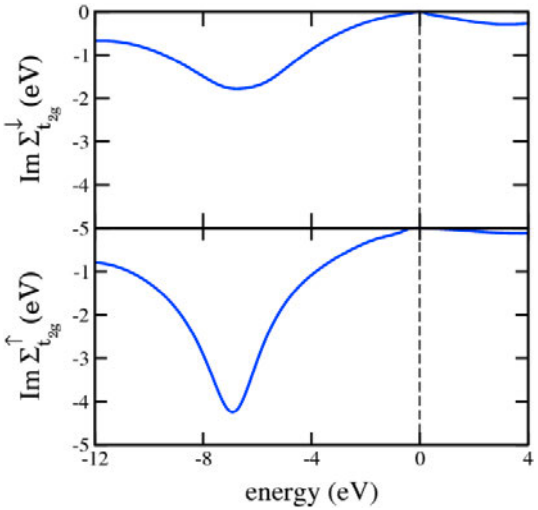

Bloch spectral function

Band structure of fcc-Ni $\vec{k}$ along Γ-X

LSDA
dispersion relation

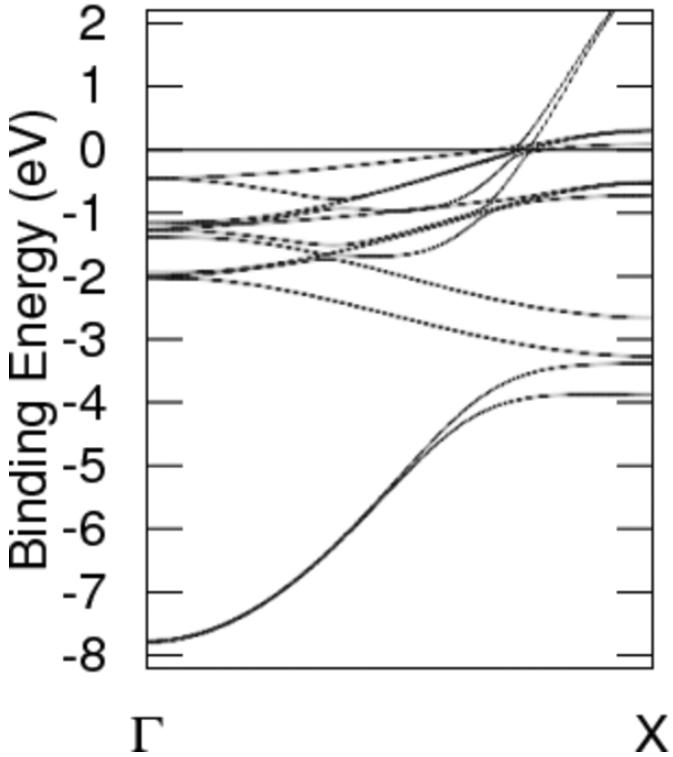

LSDA+DMFT
Bloch spectral function

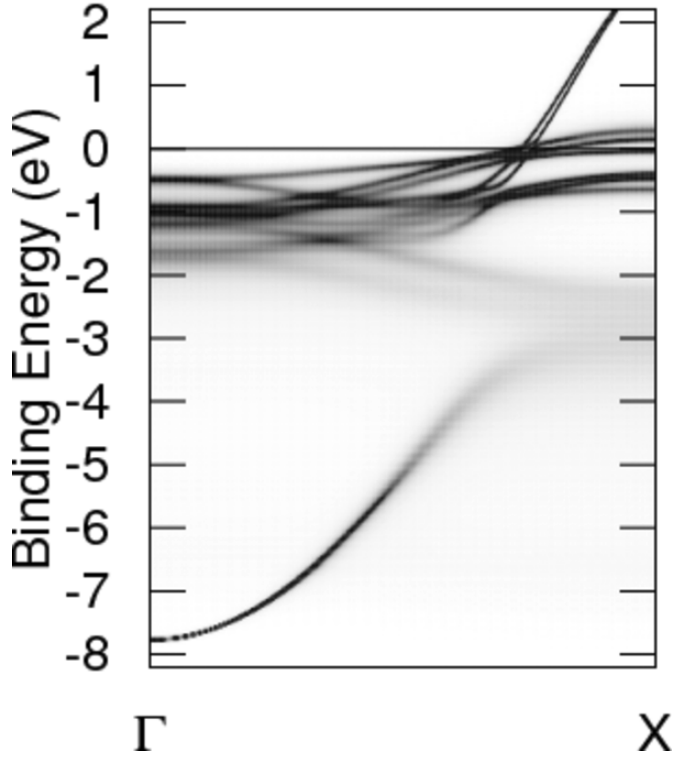

Bloch spectral function

$$A_{\mathrm{B}}(\vec{k},E) = -\frac{1}{\pi}\sum_{n}^{N} e^{-\imath\vec{k}\vec{R}_n} \Im \int_{\Omega} d^3r \left\langle G\left(\vec{r},\vec{r}+\vec{R}_n,E\right)\right\rangle$$

The Dirac Equation for magnetic solids

$$\left[\frac{\hbar}{i}c\vec{\alpha}\cdot\vec{\nabla}+\beta mc^2+\bar{V}(\vec{r})+\underbrace{\beta\vec{\sigma}\cdot\vec{B}_{\mathrm{eff}}(\vec{r})}_{V_{\mathrm{spin}}(\vec{r})}\right]\Psi(\vec{r},E)=E\,\Psi(\vec{r},E)$$

effective magnetic field

$$\vec{B}_{\mathrm{eff}}(\vec{r})=\frac{\partial E_{\mathrm{xc}}[n,\vec{m}]}{\partial\vec{m}(\vec{r})}$$

is determined by the spin magnetisation $\vec{m}(\vec{r})$
within **spin density functional theory (SDFT)**

Within an atomic cell one can choose $\hat{\mathbf{z}}'$ to have:

$$V_{\mathrm{spin}}(\vec{r})=\beta\sigma_{z'}\,B_{\mathrm{eff}}(r)$$

Ansatz to solve the single site Dirac equation

$$\psi_\nu(\vec{r}, E) = \sum_\Lambda \psi_{\Lambda\nu}(\vec{r}, E)$$

with

$$\psi_{\Lambda\nu}(\vec{r}, E) = \begin{pmatrix} g_{\Lambda\nu}(r, E)\, \chi_\Lambda(\hat{\vec{r}}) \\ i f_{\Lambda\nu}(r, E)\, \chi_{-\Lambda}(\hat{\vec{r}}) \end{pmatrix}$$

spin-angular function

$$\chi_\Lambda(\hat{r}) = \sum_{m_s=\pm 1/2} C(l\tfrac{1}{2}j; \mu - m_s, m_s)\, Y_l^{\mu - m_s}(\hat{r})\, \chi_{m_s}$$

short hand notation $\Lambda = (\kappa, \mu)$ and $-\Lambda = (-\kappa, \mu)$

Dirac Equation within LSDA+DMFT

$$\left[\frac{\hbar}{i}c\vec{\alpha}\cdot\vec{\nabla}+\beta mc^2+\bar{V}(\vec{r})+\underbrace{\beta\sigma_z\cdot B_{\mathrm{eff}}(\vec{r})}_{V_{\mathrm{spin}}(\vec{r})}-E\right]\Psi(\vec{r})$$

$$+\int d^3r'\Sigma(\vec{r},\vec{r}',E)\,\Psi(\vec{r}')=0$$

$$\vec{B}_{\mathrm{eff}}(\vec{r})=\frac{\partial E_{\mathrm{xc}}[n,\vec{m}]}{\partial\vec{m}(\vec{r})}$$

is determined by the spin magnetisation $\vec{m}(\vec{r})$
within **spin density functional theory (SDFT)**

Relativistic LSDA+DMFT scheme

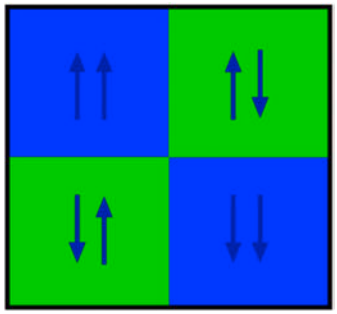

$$(H_0 + V_\uparrow + \Sigma_{\uparrow\uparrow})\,\psi_\uparrow + \left(h^{\mathrm{SOC}}_{\uparrow\downarrow} + \Sigma_{\uparrow\downarrow}\right)\psi_\downarrow = \varepsilon_\uparrow \psi_\uparrow$$

$$(H_0 + V_\downarrow + \Sigma_{\downarrow\downarrow})\,\psi_\downarrow + \left(h^{\mathrm{SOC}}_{\downarrow\uparrow} + \Sigma_{\downarrow\uparrow}\right)\psi_\uparrow = \varepsilon_\downarrow \psi_\downarrow$$

3d transition metals:

- orbital magnetic moments [c]
- magneto-optics of 3*d* TM conductivity, Kerr effect [c]
- photoemission of 3*d* TM Fano effect, ARPES [c]

actinides:

- magnetic moments

  $\mu_{\mathrm{spin,orbital}} = 0$ in Pu [a,b]
- phase transitions:

  α-δ-ε– transitions in Pu [a]
- photoemission:

  "3-peak"--structure in Pu [a,b]

[a] Savrasov, Kotliar, Abrahams
[b] Pourovskii, Katsnelson, Lichtenstein
[c] Perlov, Chadov, Minár, Ebert, Chioncel, Lichtenstein, Katsnelson

Relativistic self-energy matrix

3d-electron systems (Ni)

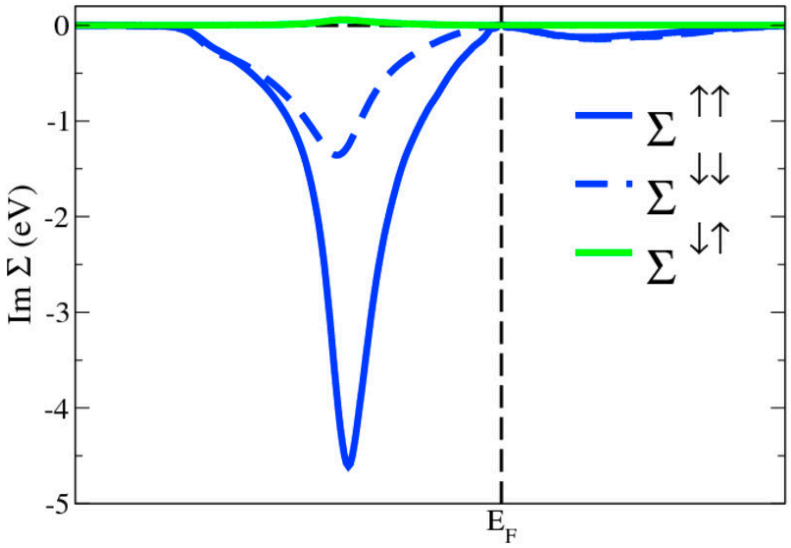

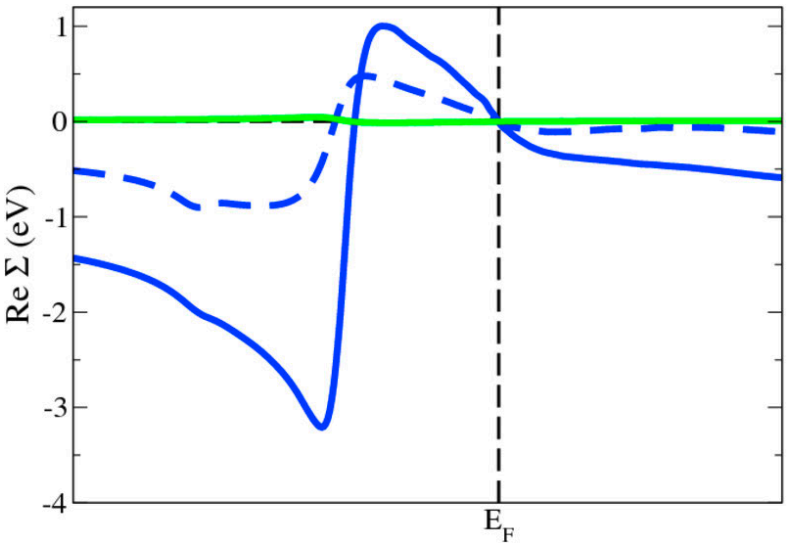

unpublished

5f-electron systems (US)

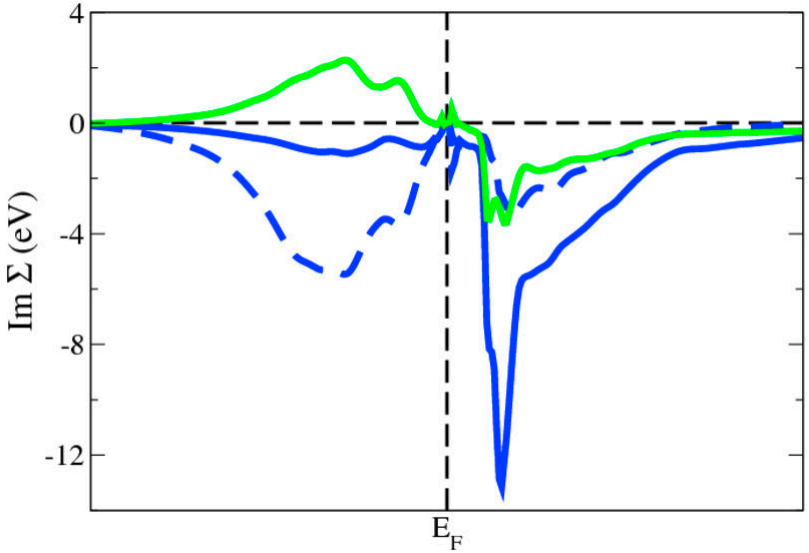

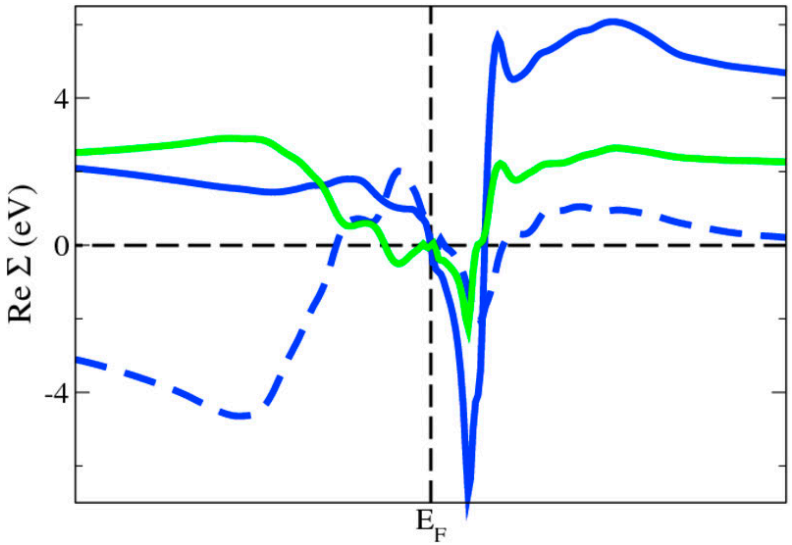

Coherent Potential Approximation - CPA

- effective CPA medium represents the electronic structure of an configurationally averaged substitutionally random alloy A_xB_{1-x}

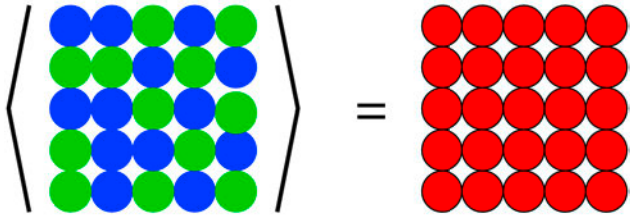

- use mean field description – find best possible single-site scheme

Embedding of an A- or B-atom into the CPA-medium
- in the average - should not give rise to additional scattering

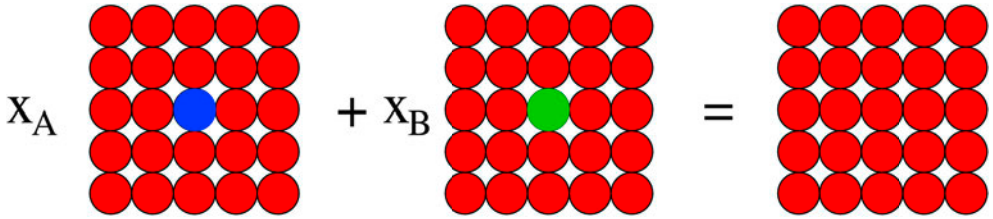

$$x_A \underline{\tau}_A^{nn} + x_B \underline{\tau}_B^{nn} = \underline{\tau}_{CPA}^{nn}$$

with the projected scattering path operator $\underline{\tau}_\alpha^{nn}$

Soven, Physical Review **156**, 809 (1967)

CPA calculations for Fe_xNi_{1-x} alloy

Spin magnetic moments

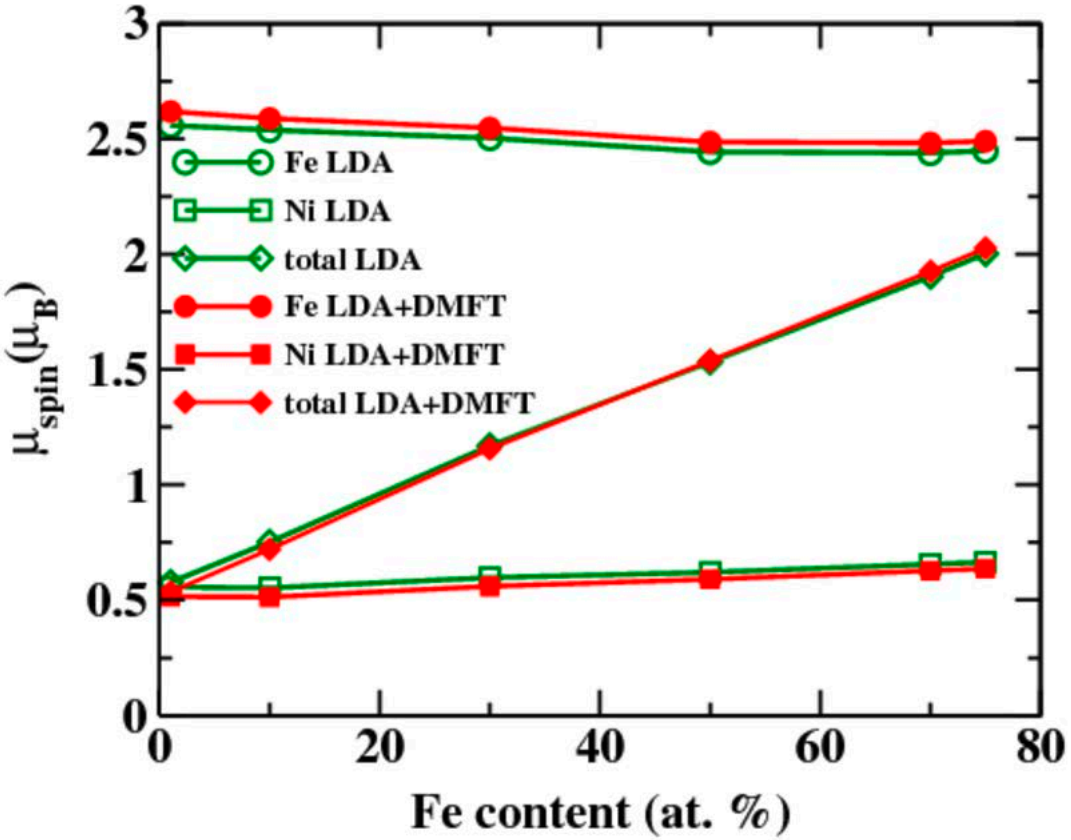

real part of Σ

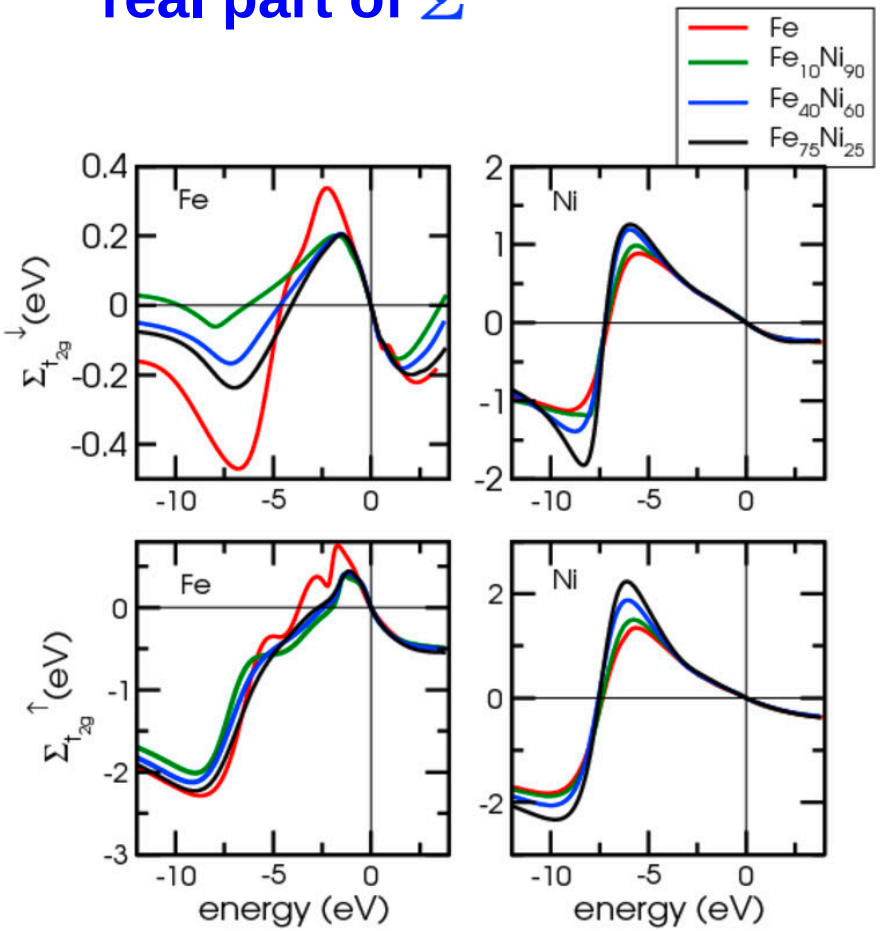

J. Minar *et al.*, PRB **72**, 045125 (2005)

Bloch spectral function of Ni_xPd_{1-x}

LSDA

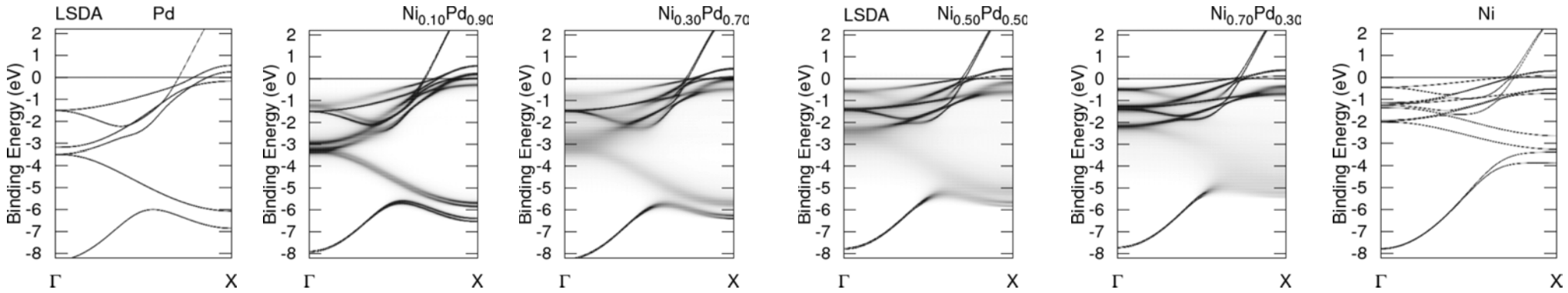

LSDA+DMFT

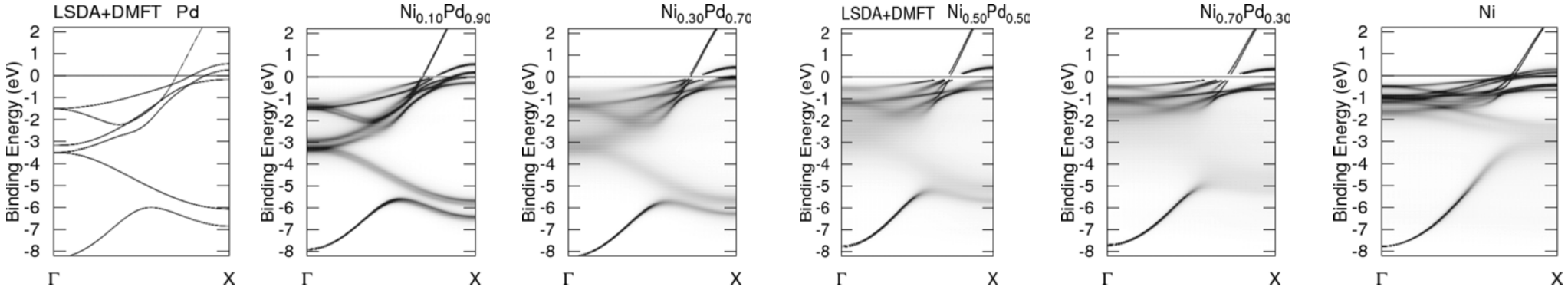

J. Braun *et al.*, PRB **82**, 024411 (2010)

Magnetic moments of Fe, Co and Ni

spin-moments

orbital-moments

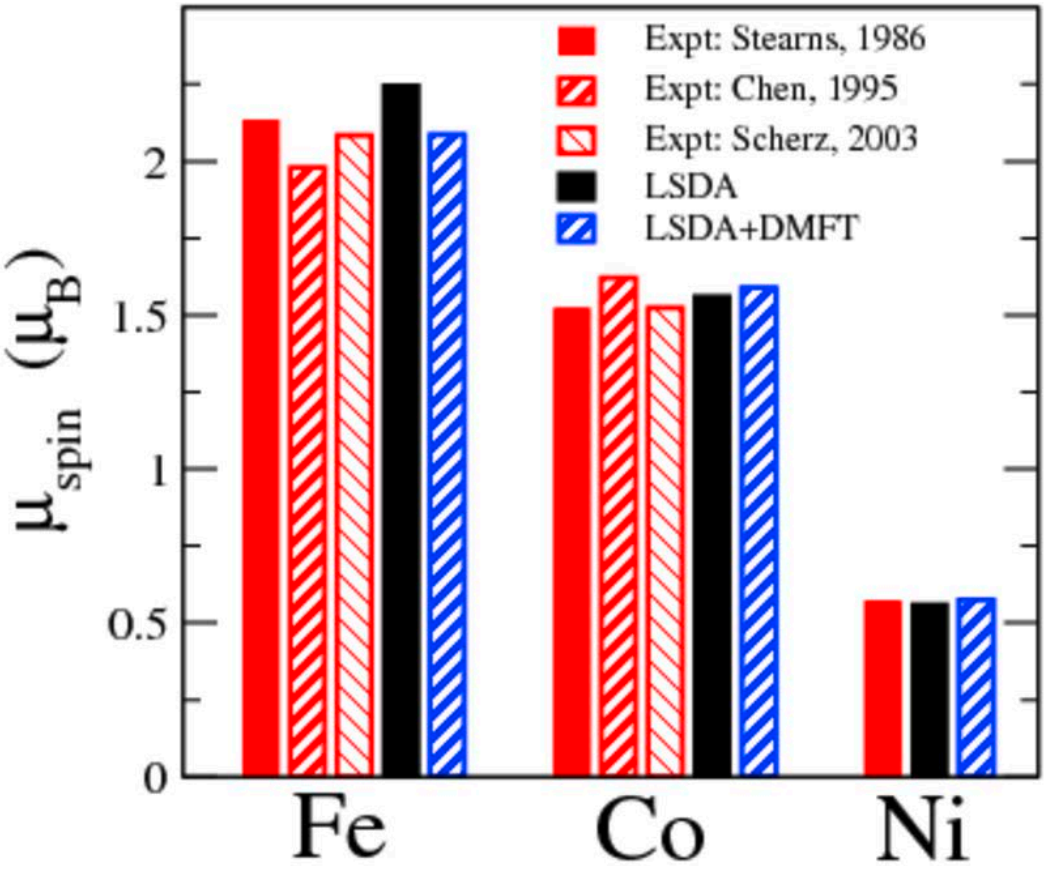

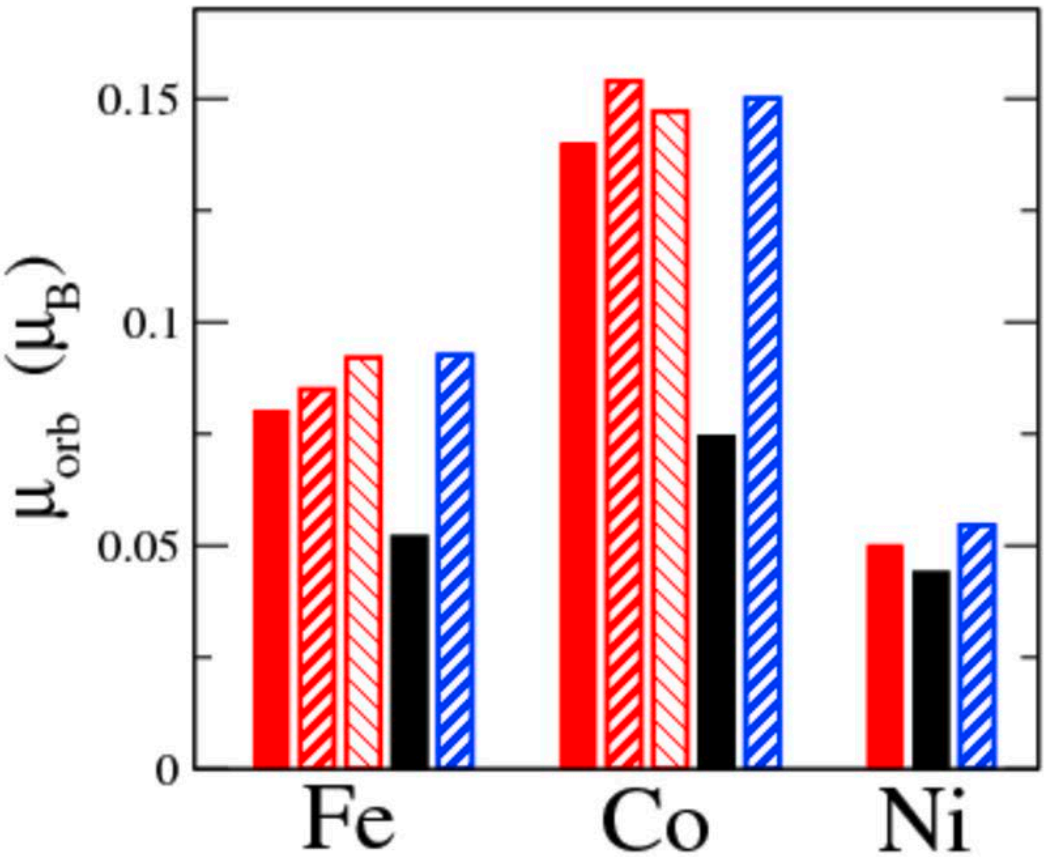

S. Chadov *et al*., EPL **82**, 37001 (2008)

Double counting

$$\Sigma_{12}^{\mathrm{LSDA+DMFT}}(\omega)$$
$$= \Sigma_{12}^{\mathrm{LSDA+DMFT}}(\omega) - \Sigma_{12}^{\mathrm{LSDA+DMFT}}(\omega = 0) + \Sigma_{12}^{\mathrm{LSDA+U}}(\omega = 0)$$

$$\Sigma_{12}^{\mathrm{LSDA+U}} = \sum_{34} \{U_{1234} - U_{1342}\} n_{34} - \delta_{12}\Sigma_{12}^{\mathrm{DC}}$$

$$< n >_\sigma = \frac{1}{2}$$

$$< n >_\sigma = \frac{1}{2l+1} \sum_{m=-l}^{l} n_{mm}^{\sigma\sigma}$$

Atomic limit (fully localised limit)

$$\Sigma_{11}^{\mathrm{AL-DC}} = U\left(N - \frac{1}{2}\right) + J\left(N_{\sigma_1} - \frac{1}{2}\right)$$

Around meanfield

$$\Sigma_{11}^{\mathrm{AMF-DC}} = U(N - < n >_{\sigma_1}) - J(N_{\sigma_1} - < n >_{\sigma_1})$$

(111)-surface of fcc-Ni

LSDA+DMFT-based layer-resolved results

self-energy

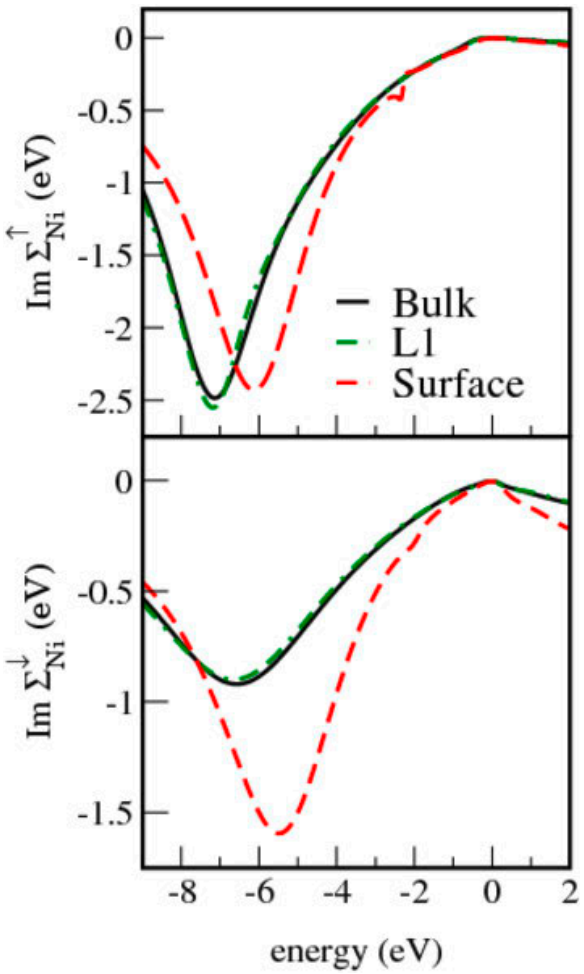

Spin and orbital magnetic moments

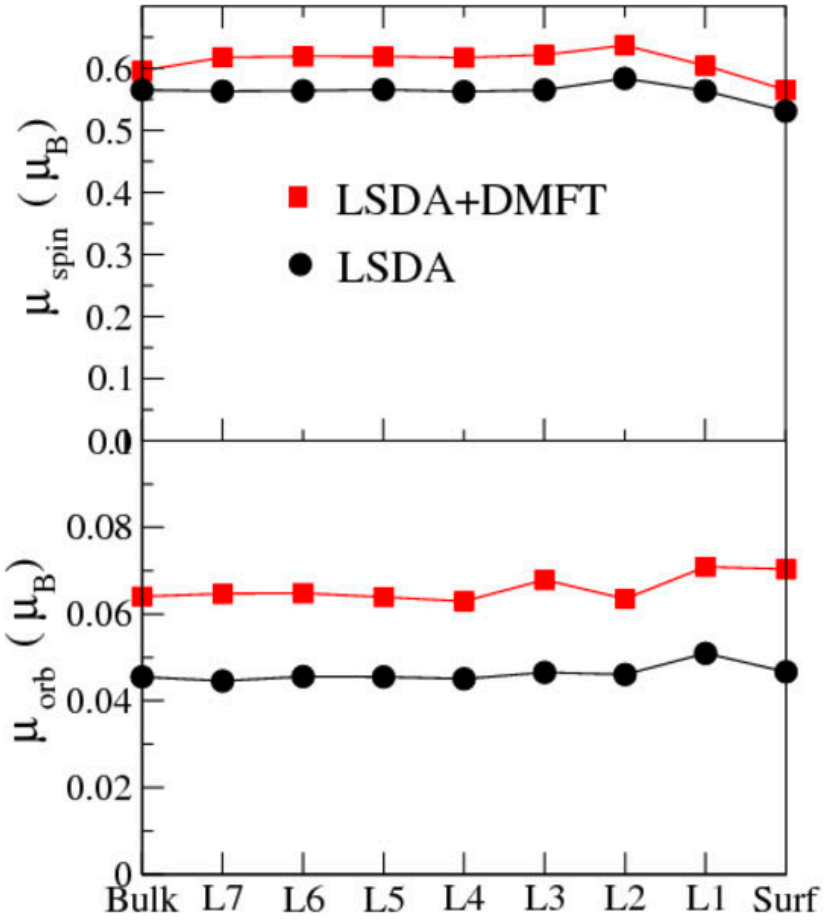

unpublished

Magnetic moments of bcc Fe_xCo_{1-x}

Comparison of LSDA-, LSDA+OP- and LSDA+DMFT-based results with experiment

Spin

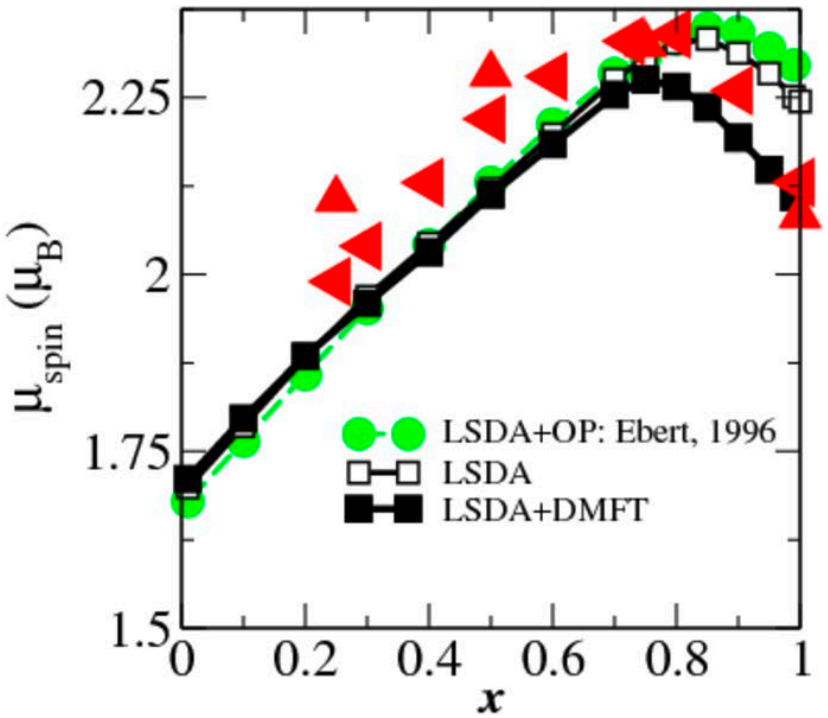

Orbital

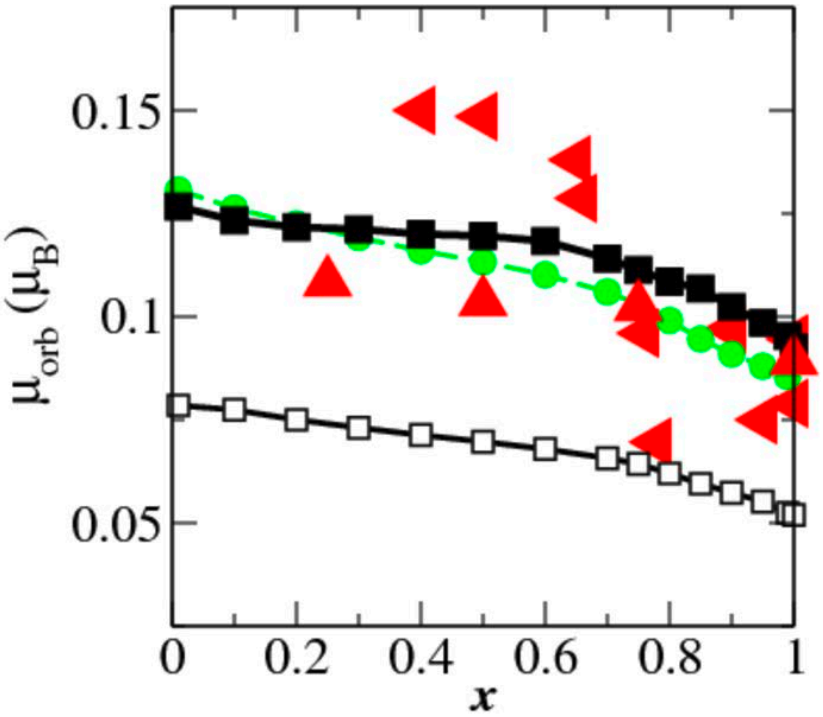

- Strong enhancement of orbital moments

S. Chadov *et al*. EPL **82**,37001 (2008)

Total energy of fcc Ni

KKR+DMFT

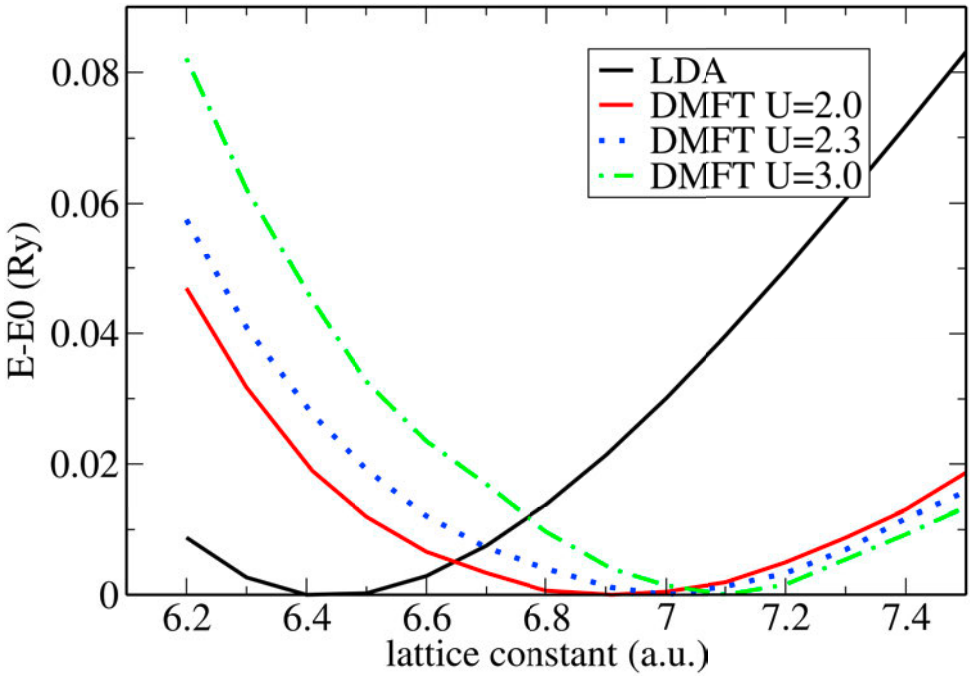

U=2eV J=0.9eV	volume $(a.u.)^3$	bulk mod. (GPa)
LSDA	66.86	280
DMFT (LMTO)	76.20	163
DMFT (KKR)	76.28	171
Expt.	73.52	186

I. Di Marco et al., PRB **79**, 115111 (2009)

Spin- and Angle-resolved photoemission

radiation source
wave vector $\vec{q}$
polarisation λ

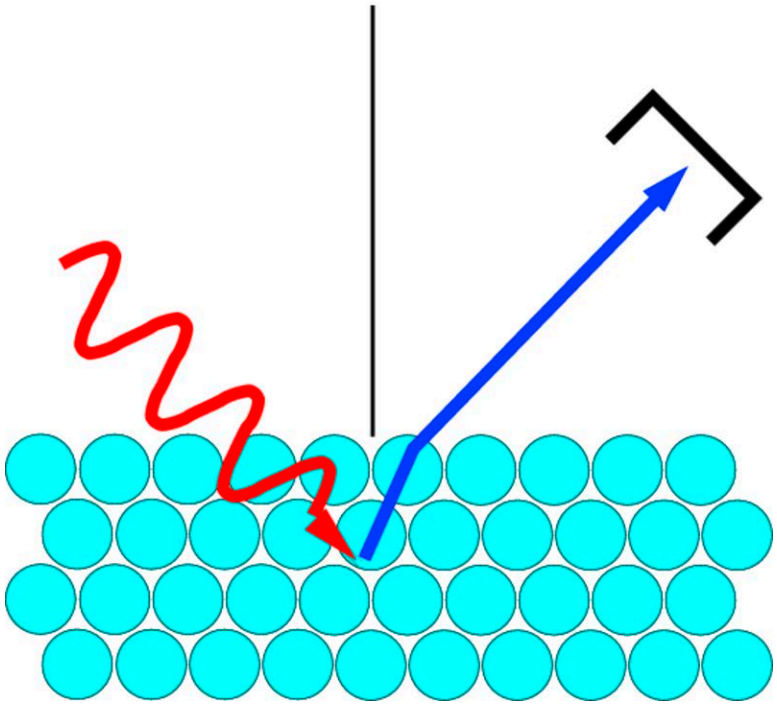

photo electron detector
wave vector $\vec{k}$
spin state m_s

photo current

$$j^{\vec{q}\lambda}_{\vec{k}m_s}(E+\omega) \propto \int d^3r_1 \int d^3r_2 \left[\mathcal{T}_R \phi^{\mathrm{LEED}}_{\vec{k}m_s}(\vec{r}_1, E+\omega)\right]^{\dagger} X_{\vec{q}\lambda}(\vec{r}_1)$$

$$\Im G(\vec{r}_1, \vec{r}_2, E)\, X^{\dagger}_{\vec{q}\lambda}(\vec{r}_2)\, \mathcal{T}_R \phi^{\mathrm{LEED}}_{\vec{k}m_s}(\vec{r}_2, E+\omega)$$

$$\phi^{\mathrm{LEED}}_{\vec{k}m_s}(\vec{r}, E) = \Xi_{m_s} e^{i\vec{k}\vec{r}} + \int d^3r'\, G(\vec{r}, \vec{r}', E)\, V(\vec{r}')\, \Xi_{m_s} e^{i\vec{k}\vec{r}'}$$

Fano effect in VB-photoemission

Spin polarisation of photo electrons
due to spin-orbit coupling

spin-resolved angle-integrated photoemission experiment

ferromagnetic systems

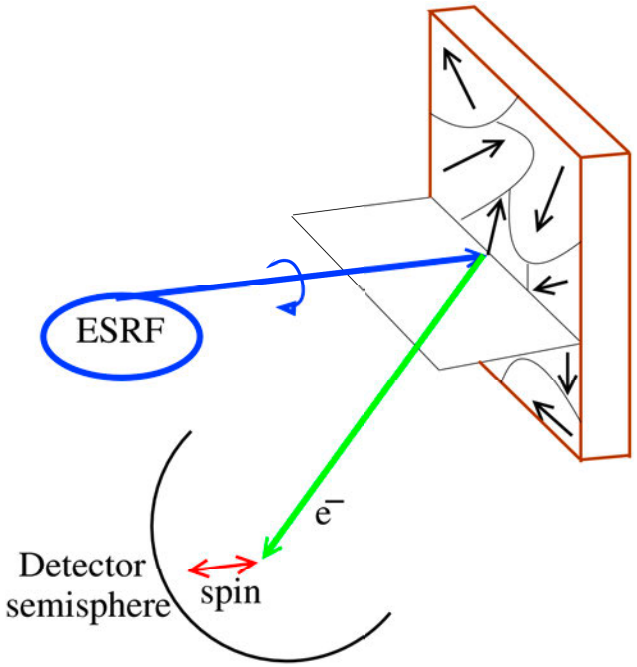

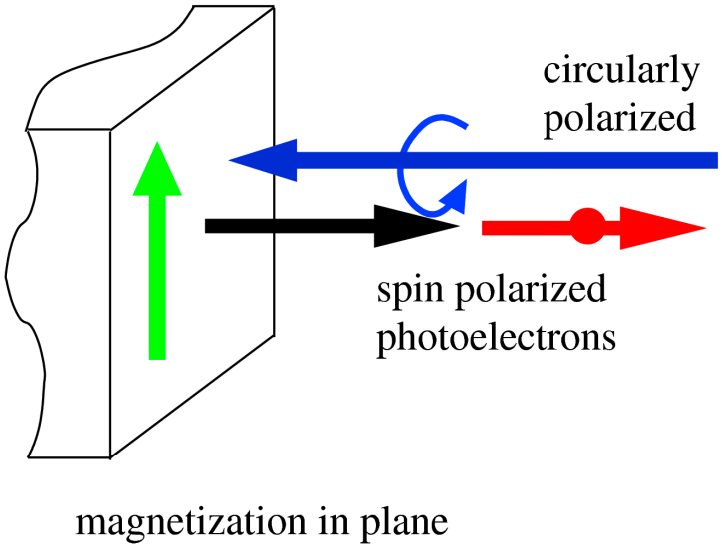

Fano effect in VB-XPS of ferromagnets

Photocurrent and spin-difference $E_{phot} = 600$ eV

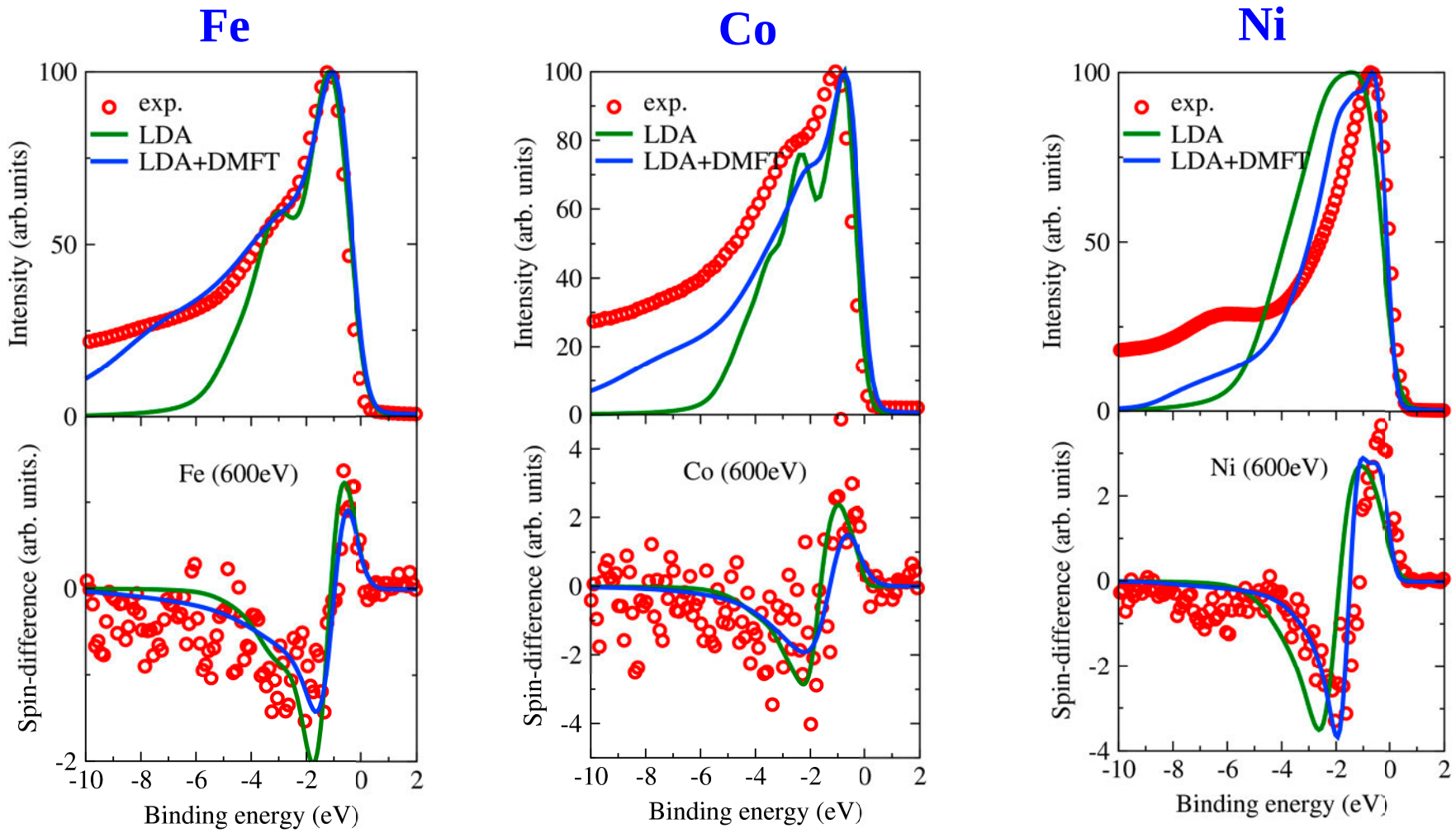

Minár *et al*., PRL **95**, 166401 (2005) - Experiments - N. Brookes *et al*., ESRF

ARPES of Ni (110)

Comparison between experiment and theory

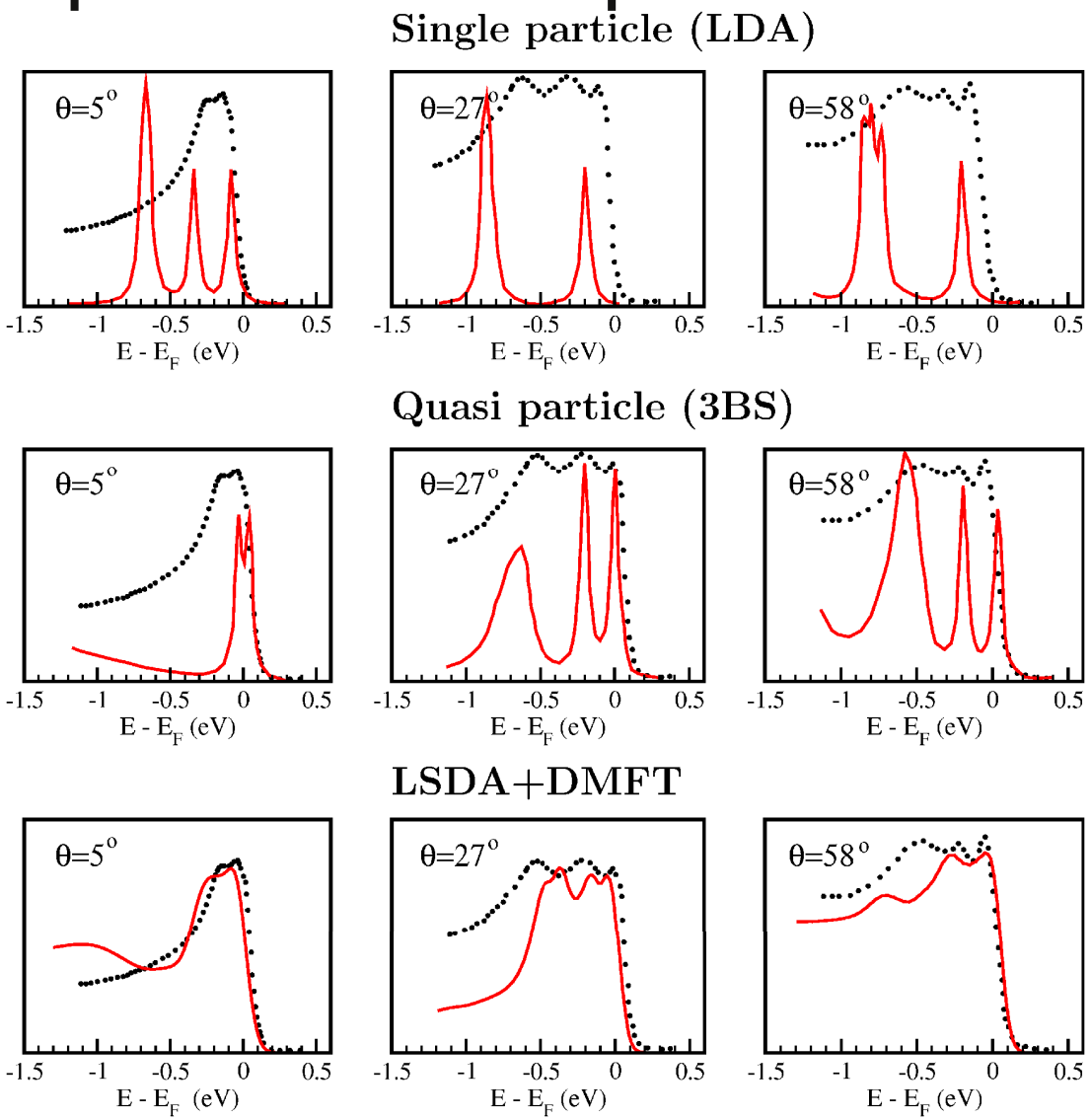

Spin-resolved spectra

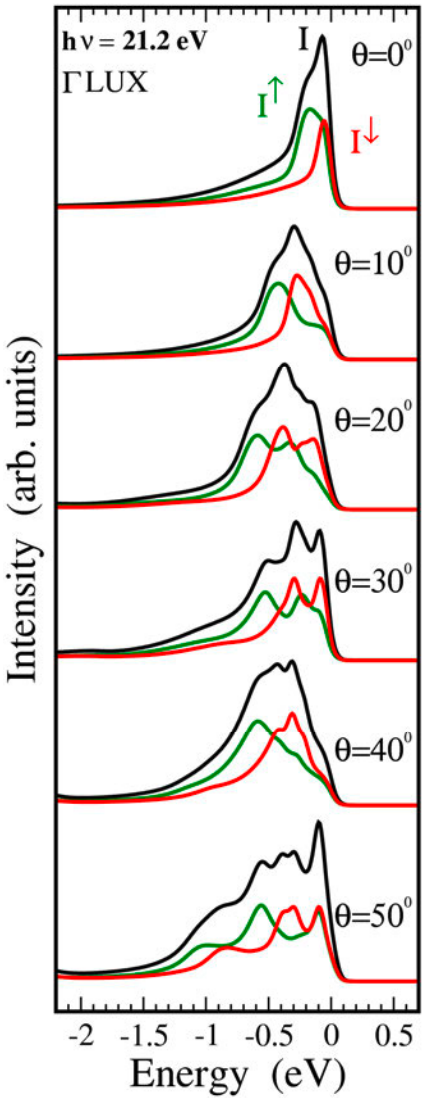

3BS, Exp: F. Manghi, J. Osterwalder *et al.* PRB **59**, R10409 (1999)
LSDA+DMFT: J. Braun et al., PRL **97**, 227601 (2006)

Electronic structure and ARUPS of Fe(110)

Bloch spectral functions

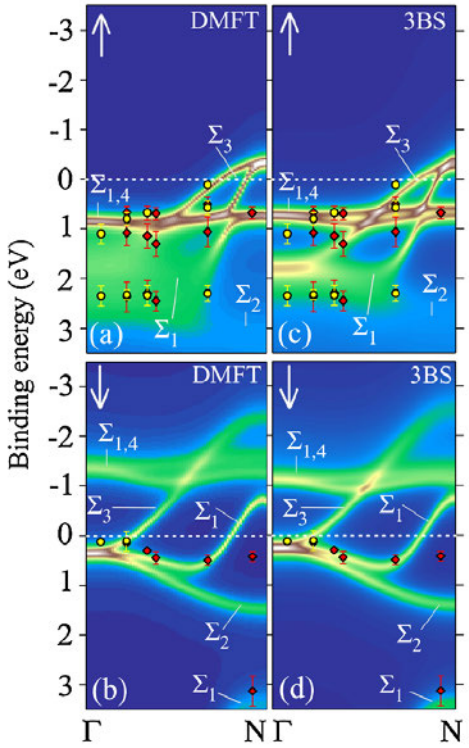

- U=1.5eV, J=0.9eV
- Agreement between

  3BS (F. Manghi) and DMFT
- Tamm resonance (close to E_F)
- Quantitative agreement for complete BZ along ΓN

Normal emission along ΓN (E_{phot}=26-80eV)

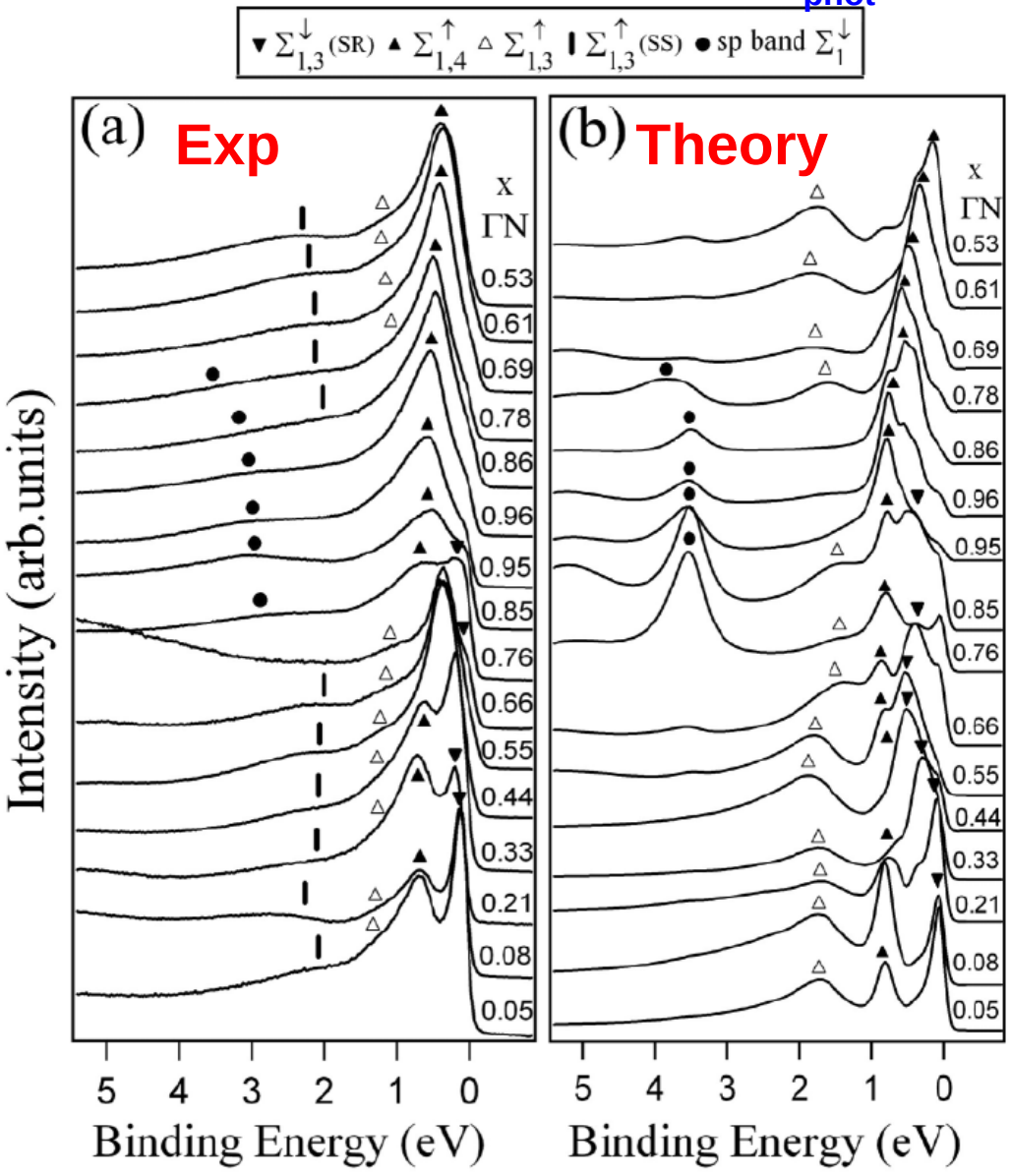

J.S. Barriga, Minar et al. PRL 103, 267203 (2009)

Spin integrated spectra for Fe, Co and Ni

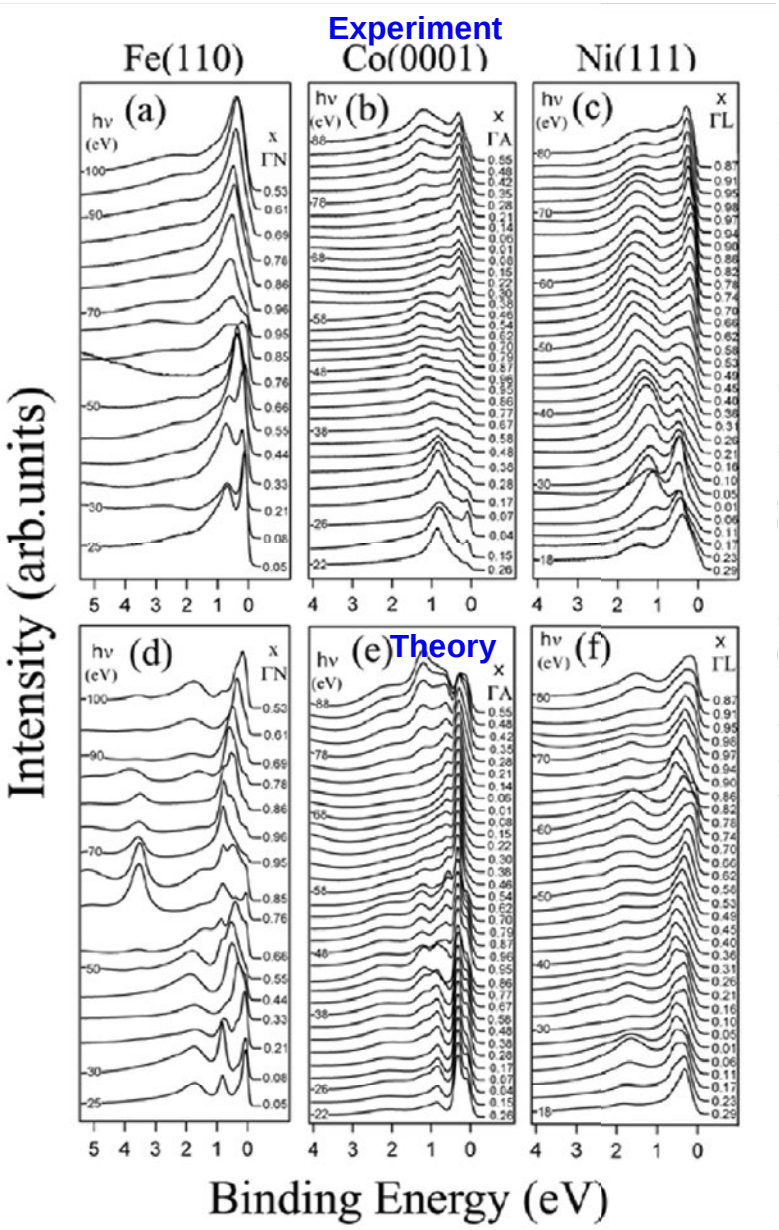

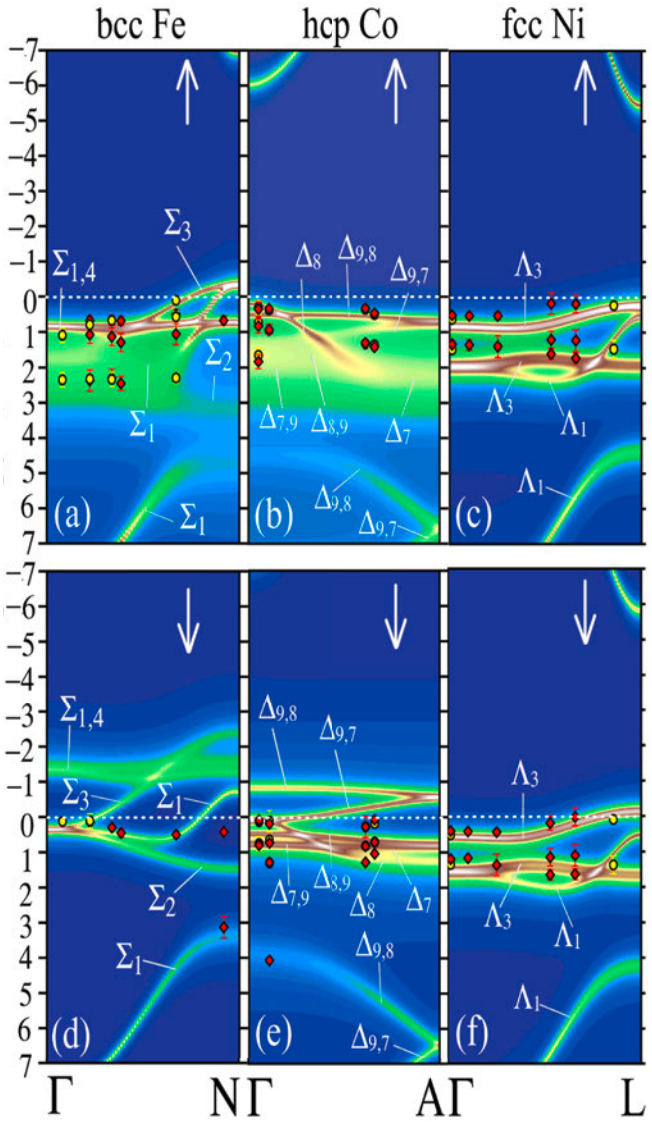

Fe Co Ni

Averaged U

Non-local correlations

- LSDA+DMFT: improved description of spectroscopic data from 3d-ferromagnets
- Normal emission, p-pol light
- U_{Fe}= 1.5 eV, U_{Co}= 2.5 eV, U_{Ni}= 2.8 eV
- Need for non-local correlations

Minar; Braun et al, PRB in preparation (2011)

Long standing problems of LSDA in Ni

Fano effect
Angle integrated PES

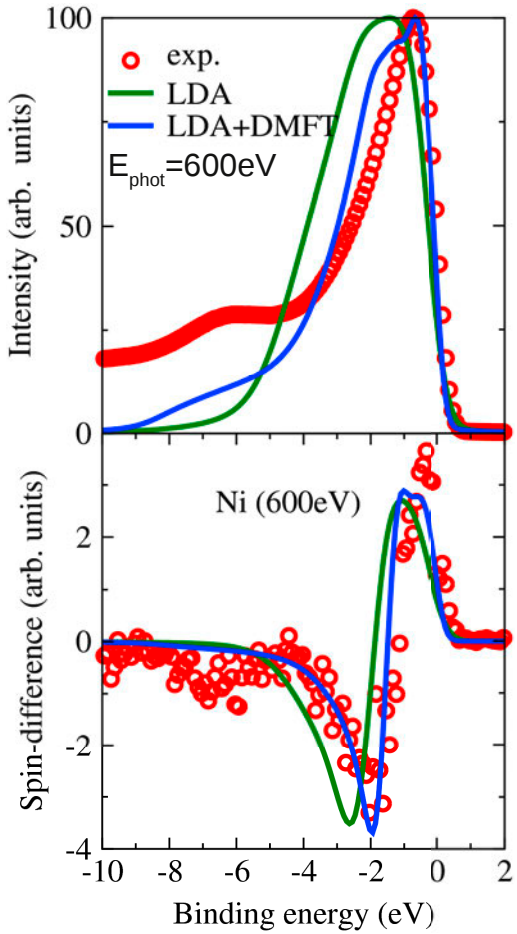

Minar et al,
PRL 95, 166401 (2005)

Soft X-PES
Fermi surface

LSDA

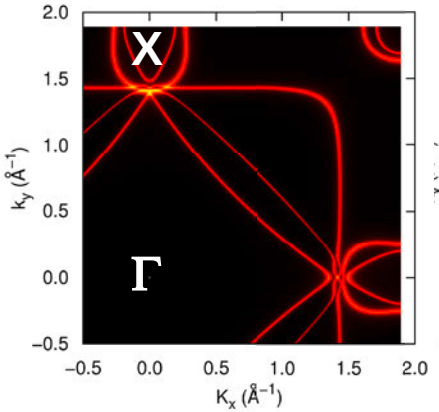

LSDA+DMFT

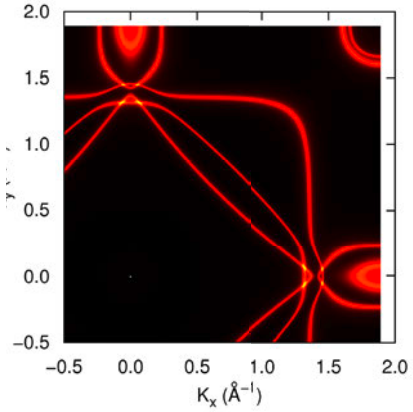

Exp.

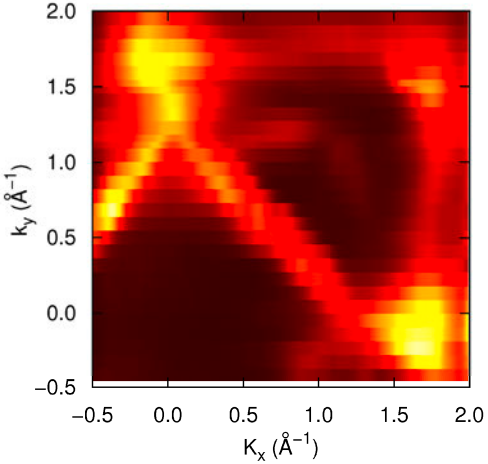

Minar, Braun, Chainani, Shin et al,
PRL, submitted (2011)

6eV Satellite
in normal emission

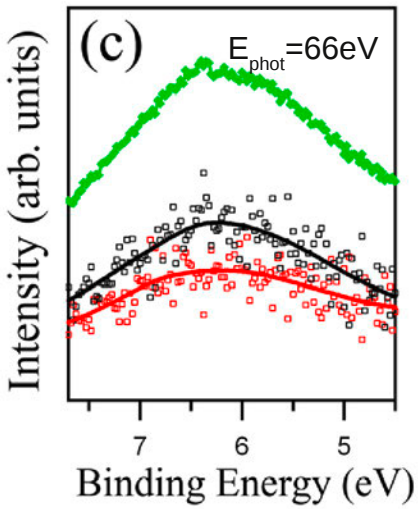

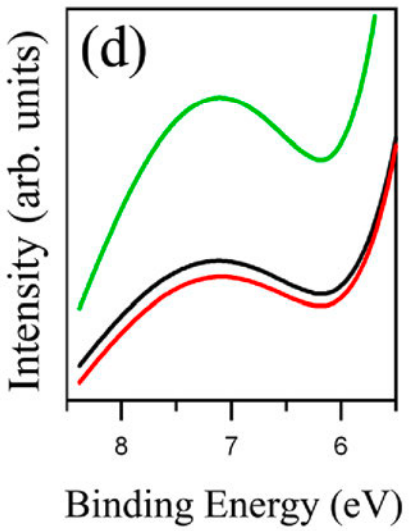

Barriga et al,
PRB, in preparation (2011)

Magnetic Compton scattering

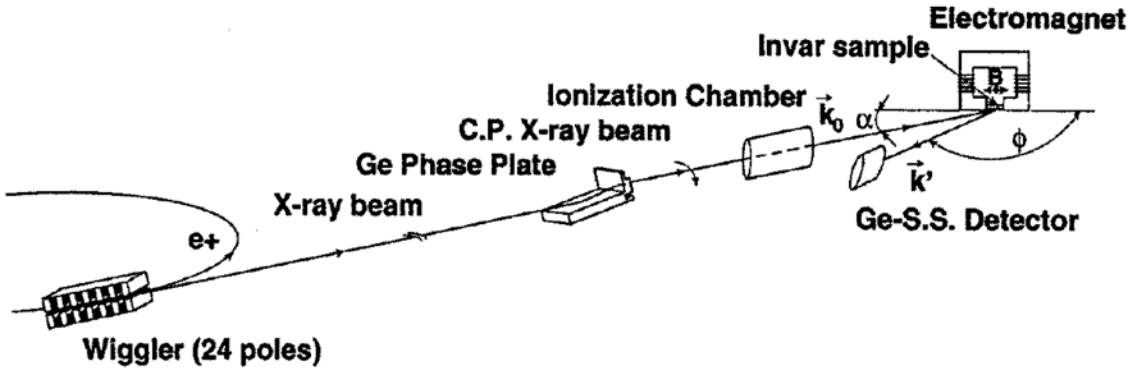

Spin contribution in cross-section

$$\left(\frac{\partial^2\sigma}{\partial\Omega\partial p_z}\right)_{\uparrow} - \left(\frac{\partial^2\sigma}{\partial\Omega\partial p_z}\right)_{\downarrow} = P_c r_0^2 \left(\frac{k'}{k_0}\right)^2 \Psi_2(\vec{\sigma}) J_{spin}(p_z)$$

Geometry factor

$$\Psi_2 = \pm\sigma\left(k_o \cos\alpha\cos\phi - k'\cos(\alpha-\phi)\right) \times (\cos\phi - 1)\frac{\hbar c}{m_o c^2}$$

Magnetic Compton profile

$$J_{spin}(p_z) = \int\int \left(n^{\uparrow}(\vec{p}) - n^{\downarrow}(\vec{p})\right) dp_x dp_y$$

Magnetic Compton profile for Fe and Ni

Fe along [111] direction

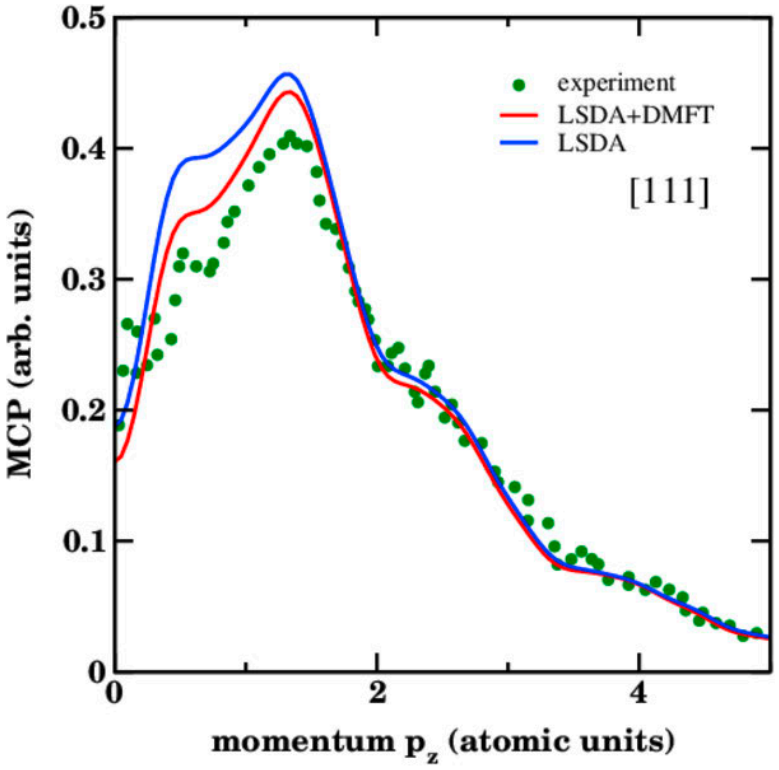

Ni along [111] direction

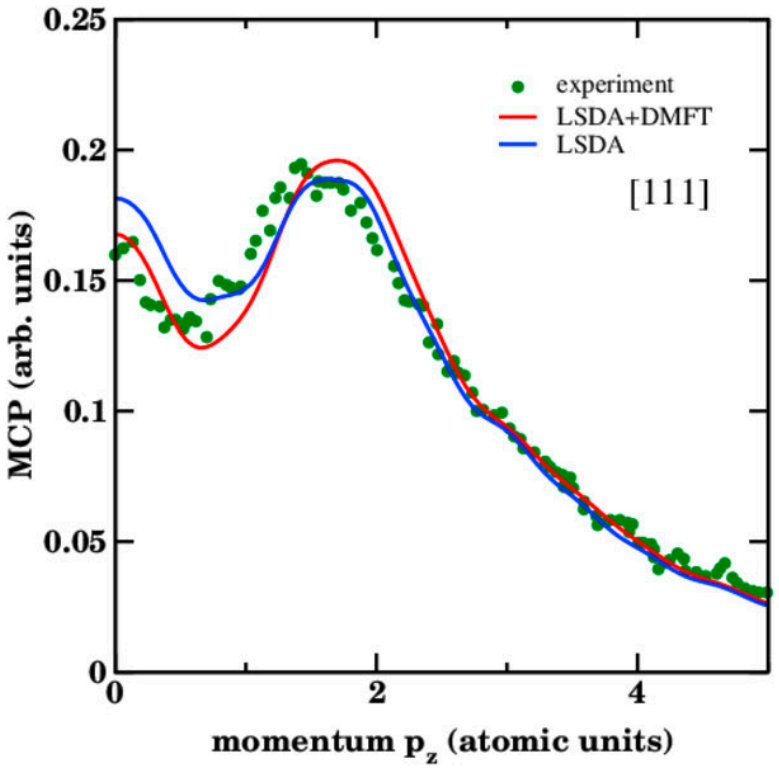

- MCP ==> direct measure of the ground state spin density
- LSDA+DMFT calculations for U= 2.3eV, J= 0.9eV
- Experimental Data: McCarthy et al., jsr (1997), Dixon et al., jpcm (1998)
- Considerable improvement in low momentum regime

6eV satellite contribution to MCP for Ni

Density of states

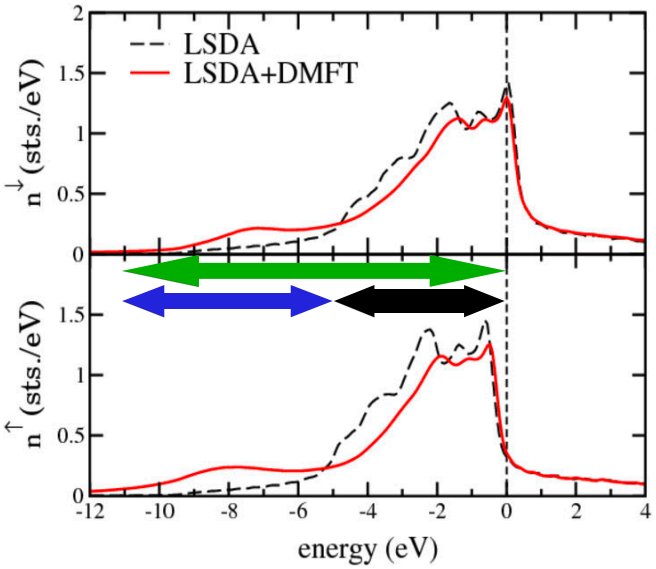

LSDA

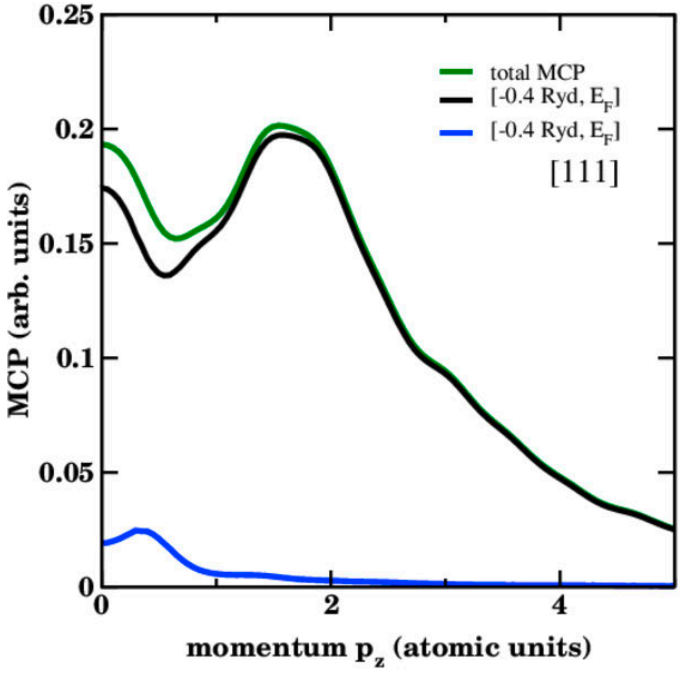

LSDA+DMFT

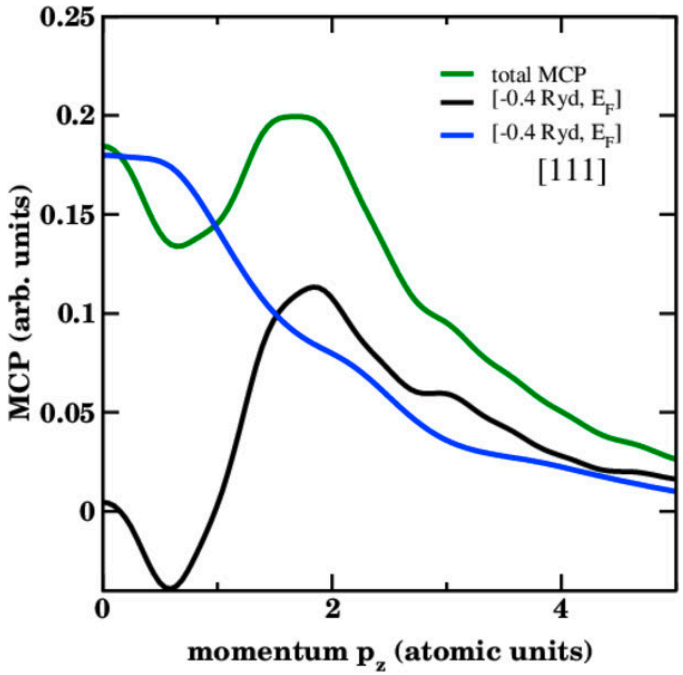

- LSDA+DMFT calculations for U= 2.3eV, J= 0.9eV
- Signature of spin polarized 6eV satellite
- Broad contribution of 6eV satellite ==> localized states
- Similar contribution observed in various directions ==> localized states

Summary

- Combination of KKR-method and LSDA+DMFT
  - alloys
  - inhomogeneous systems
  - spectroscopy
- Direct comparison to experiment allows to check in particular
  - Accuracy of DMFT solver
  - Value of parameters U and J
  - Type of double counting
- Examples presented
  - Spin and magnetic moments
  - Equilibrium lattice properties via total energy
  - Angle resolved photo emission
  - Magnetic Compton scattering